

Measurements of radio propagation in rock salt for the detection of high-energy neutrinos

Amy Connolly^a, Abigail Goodhue^b, Christian Miki^c,
Ryan Nichol^a, David Saltzberg^b

^a*Department of Physics and Astronomy, University College London, Gower Street,
London WC1E 6BT UK*

^b*Department of Physics and Astronomy, UCLA, 475 Portola Plaza,
Mailstop 154705, Los Angeles, CA 90095-1547 USA*

^c*Department of Physics and Astronomy, University of Hawaii, 2505 Correa Rd.,
Honolulu, HI 96822 USA*

Abstract

We present measurements of the transmission of radio/microwave pulses through salt in the Cote Blanche salt mine operated by the North American Salt Company in St. Mary Parish, Louisiana. These results are from data taken in the southwestern region of the 1500 ft. (457 m) deep level of the mine on our third and most recent visit to the mine. We transmitted and received a fast, high-power, broadband pulse from within three vertical boreholes that were drilled to depths of 100 ft. (30 m) and 200 ft. below the 1500 ft. level using three different pairs of dipole antennas whose bandwidths span 125 to 900 MHz. By measuring the relative strength of the received pulses between boreholes with separations of 50 m and 169 m, we deduce the attenuation of the signal attributed to the salt medium. We fit the frequency dependence of the attenuation to a power law and find the best fit field attenuation lengths to be 93 ± 7 m at 150 MHz, 63 ± 3 m at 300 MHz, and 36 ± 2 m at 800 MHz. This is the most precise measurement of radio attenuation in a natural salt formation to date. We assess the implications of this measurement for a future neutrino detector in salt.

Key words: salt, radio, microwave, transmission, attenuation, neutrino

PACS: 42.25.Bs, 91.55.De, 93.85.Fg, 95.85.Ry

Email address: amyc@hep.ucl.ac.uk (Amy Connolly).

1 Introduction

2 The observation of cosmic rays with energy higher than the Greisen-Zatsepin-
3 Kuzmin (GZK) cutoff at $\sim 10^{19.5}$ eV [1] implies a corresponding flux of ultra
4 high-energy (UHE) neutrinos, with energy in the $10^{17} - 10^{19}$ eV range [2].
5 These secondary neutrinos are created via photomeson production of cosmic
6 rays on the 2.7 K cosmic microwave background. Detection of these neutrinos
7 would provide unique information about the origin of primary cosmic rays and
8 the nature of their sources.

9 Although predictions for the flux of UHE neutrinos differ by orders of mag-
10 nitude, a reasonable set of parameters puts the rate of UHE neutrinos at the
11 level of $10/\text{km}^2/\text{century}$ [2]. A detector volume of hundreds of cubic kilometers
12 water equivalent is required to detect a significant number of neutrinos in this
13 energy regime. Optical techniques are widely used in neutrino detectors, but
14 the volume that can be instrumented is constrained by attenuation lengths of
15 tens of meters at optical frequencies in detector media (such as ice), so optical
16 detectors have limited sensitivity to rare high-energy events.

17 G. Askaryan first predicted coherent radio emission from ultra high-energy
18 showers [4], and the effect has been confirmed in accelerator beam tests [5].
19 The energy of the coherent radio emission that results from the development of
20 a negative charge excess in the shower depends quadratically on shower energy,
21 and for showers with energy greater than 10^{16} eV, dominates the emitted

22 Cherenkov power spectrum.

23 Askaryan also proposed a few materials as detection media that occur natu-
24 rally in very large volumes and are expected to have long attenuation lengths
25 in the radio regime, including ice and salt. Radio attenuation lengths longer
26 than 1 km have been measured in ice near the South Pole [3].

27 Formations of salt rock could therefore be a viable detector for high-energy
28 neutrinos if attenuation in the radio regime is indeed low. Domes of rock salt
29 occur naturally in many parts of the world, including the Gulf Coast region
30 of the United States. In these formations, the salt originates from dried ocean
31 beds which have been buoyed upward due to geological forces through a pro-
32 cess called diapirism. Through this process, the salt becomes very pure as
33 impurities are extruded. Such salt domes, with typical dimensions of several
34 square kilometers by several kilometers deep, are thought to be good candi-
35 dates for a neutrino detector. For a more detailed discussion of the dielectric
36 properties of salt and the application to neutrino detection, see Reference [6].

37 **2 Previous Measurements**

38 There are two classifications of measurements that have been made of the
39 radio properties of rock salt in salt domes. Ground Penetrating Radar (GPR)
40 was used in the 1960's and 1970's to determine the size and structure of salt
41 domes. This technique is based on sending a radar signal into the salt and

42 looking for reflections from interfaces in the salt structure. One can calcu-
43 late the distance of the interface from the time delay of the reflected pulse.
44 Although the primary purpose of the GPR measurements is to calculate in-
45 terface distances, one can also extract an attenuation coefficient based on the
46 detected signal voltage, the voltage of the transmitted pulse, and the distance
47 over which the pulse traveled. Using the GPR technique to extract attenua-
48 tion is complicated by the unknown reflection coefficient and geometry at the
49 surface of reflection, but assuming a coefficient of 1.0 from a flat surface gives
50 a conservative estimate.

51 Direct measurements of attenuation in rock salt have also been made. In 2002,
52 measurements made at Hockley salt mine showed attenuation lengths consis-
53 tent with being longer than 40 m at 150 and 300 MHz [6]. Their measurements
54 were limited by the voltage of the pulser, which limited their transmission dis-
55 tances in the salt. We decided to follow the techniques of the direct transmis-
56 sion measurements but used a high voltage pulser so that we could transmit
57 through longer distances of salt.

58 **3 Cote Blanche Salt Mine**

59 We made measurements of the dielectric properties of salt in the mine located
60 in the Cote Blanche salt dome in St. Mary Parish, Louisiana in August 2007.
61 We chose this dome because GPR measurements that were made in the mine

62 suggested very low radio attenuation, including observations of reflections over
63 the longest distance of any mine measured [7].

64 The Cote Blanche dome is one of five salt domes in the area. The salt dome
65 extends from approximately 90 m below the surface to 4270 m below the
66 surface. At a depth of 1100 ft. (335 m), the salt extends 1700 m east to west
67 and 2100 m north to south. At 2000 ft. (610 m) deep, the horizontal cross
68 section has nearly doubled in size. The total volume of salt in the dome is
69 estimated to be 28-30 km³ [8,9,10,11].

70 The dome has been actively mined since 1965 using the conventional “room
71 and pillar” method. The mine consists of a grid of 30 ft. (9 m) wide by
72 30 ft. (9 m) high drifts (corridors) spaced by 100 ft. by 100 ft. (30 m by
73 30 m) pillars of salt, and has three levels at depths of 1100 ft., 1300 ft., and
74 1500 ft. (335 m, 396 m, and 457 m). Each level covers several square kilometers.
75 Current mining operations are on the 1500 ft. deep level.

76 The measurements described in this paper are from the third trip that we
77 made to the Cote Blanche mine. In May 2005, on our first visit to the site,
78 with M. Cherry and J. Marsh from Louisiana State University, we established
79 the viability of the experimental setup and measured field attenuation lengths
80 along a corridor (within 10 meters of a wall) on the 1300 ft. level of the mine,
81 of approximately 10-15 m at 150 MHz and 300 MHz [12]. In September 2006,
82 on a return visit to the mine, we transmitted and received signals horizontally

83 across a single pillar of salt, both with antennas placed against the walls and
84 with antennas inserted 4 m into the ceiling in shallow boreholes. We measured
85 attenuation lengths of 24.6 ± 2.2 m in the frequency range 50-150 MHz, $22.2 \pm$
86 1.8 m at 150-250 MHz, and 20.5 ± 1.5 m at 250-350 MHz. We also measured
87 an average index of refraction of $n = 2.4 \pm 0.1$ [13].

88 The attenuation lengths that we measured were inconsistent with previous
89 GPR studies of the Cote Blanche mine (see Section 7). The relatively short
90 attenuation lengths that we measured through the walls of the pillar could be
91 due to the method used to mine the salt. The miners carve out corridors in
92 the salt by cutting a horizontal slice out from under the wall and then blasting
93 the section above the floor so that the salt can be removed, and then proceed
94 to a new section of salt further along the corridor. The data from our first
95 two trips were consistent with a model of very lossy salt (approximately 10 m
96 attenuation length) in the region closest to the walls of the pillar and longer
97 attenuation lengths (quoted above) in salt more than about 10 m from the
98 wall.

100 *4.1 Experimental Setup*

101 Figure 1 shows the region of the 1500 ft. deep level of the mine where we made
102 our measurements, and Figure 2 is a diagram of the experimental setup. The
103 miners drilled three 2.75 inch (7.0 cm) diameter boreholes into the salt of the
104 floor of the 1500 ft. level of the mine. Boreholes 1 and 2 were 100 ft. (30 m)
105 deep, while Borehole 3 was 200 ft. (60 m) deep. At the first two boreholes,
106 drilling was stopped at 100 ft. once the driller encountered methane gas. We
107 used a fast, high-power, broadband Pockel's cell pulser model HYP5 from
108 Grand Applied Physics with a peak voltage of 2500 kV and a 10%-90% rise
109 time of 200 ps to generate radio pulses. There was 5 ft. of LMR 240 cable
110 and 200 ft. of LMR 600 cable leading to the transmitting as well as from the
111 receiving antennas, and the antennas were lowered by hand into the salt.

112 We made most of our measurements using three pairs of dipole antennas. We
113 measured the 3 dB points of each antenna when they were in a borehole in
114 the salt to determine the in-band frequencies. The 3 dB points of the trans-
115 mission of the low frequency (LF) antenna pair (Raven Research RR6335),
116 are 50 to 175 MHz in salt. For the medium frequency (MF) antennas, which
117 we custom made, the 3 dB points are 175 and 500 MHz in salt. The high
118 frequency (HF) pair (Shure Incorporated UA820A) has a transmission band

119 between 550 and 900 MHz in salt.

120 We used a Tektronix TDS694C oscilloscope to record the received signal pulse.

121 We used a pulser with synchronized outputs to trigger both the the high-power
122 pulser and the oscilloscope. This allowed us to look in a fixed time window for
123 the signal and reduce noise by averaging many waveforms.

124 The transmitting antenna was always lowered into Borehole 1, and the iden-
125 tical receiving antenna was either in Borehole 2, which was 50 m away from
126 the transmitter, or Borehole 3, which was 169 m away from the transmitter.

127 We took data at 10 ft. (3 m) incremental depths in the boreholes. The setup
128 used to measure transmission between Boreholes 1 and 2 was identical to the
129 setup used to measure between Boreholes 1 and 3 so that we could make reli-
130 able relative measurements without requiring an absolute system calibration.

131 Because the transmission band of each antenna was relatively broad, we were
132 able to make measurements between 125 and 900 MHz in salt.

133 *4.2 Attenuation Lengths*

134 Figure 3 shows an example waveform of the received pulse at Borehole 2 and
135 Borehole 3 using the MF antennas, and Figure 4 shows the Fourier trans-
136 form of the same waveforms. To calculate the attenuation length, we first cut
137 the recorded waveforms in a time window around the pulse to eliminate any
138 reflections and reduce contributions from noise. The width of the window is

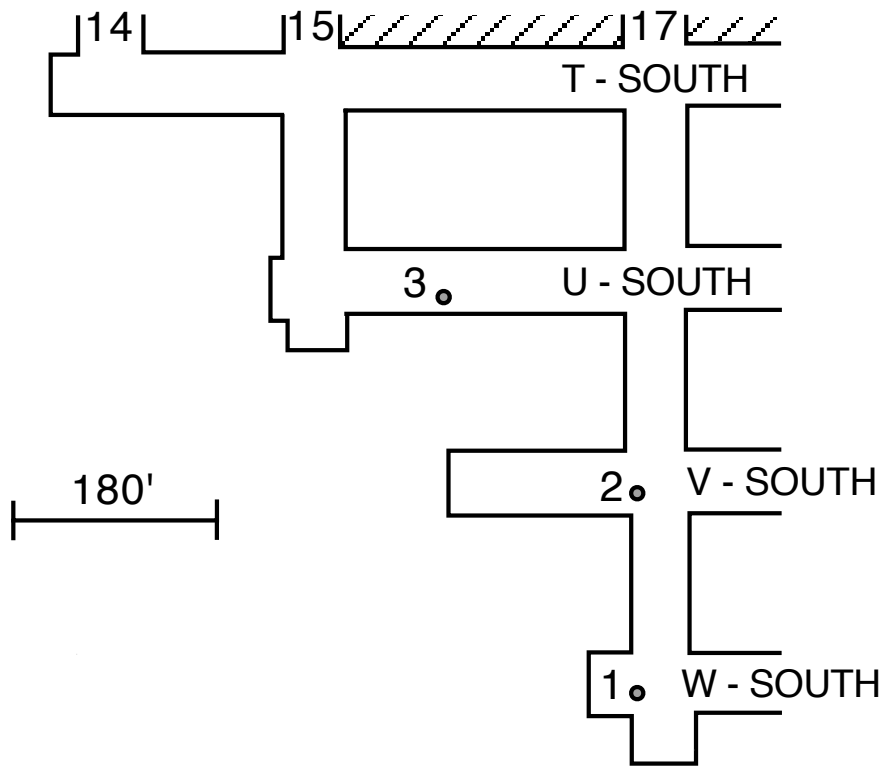


Fig. 1.

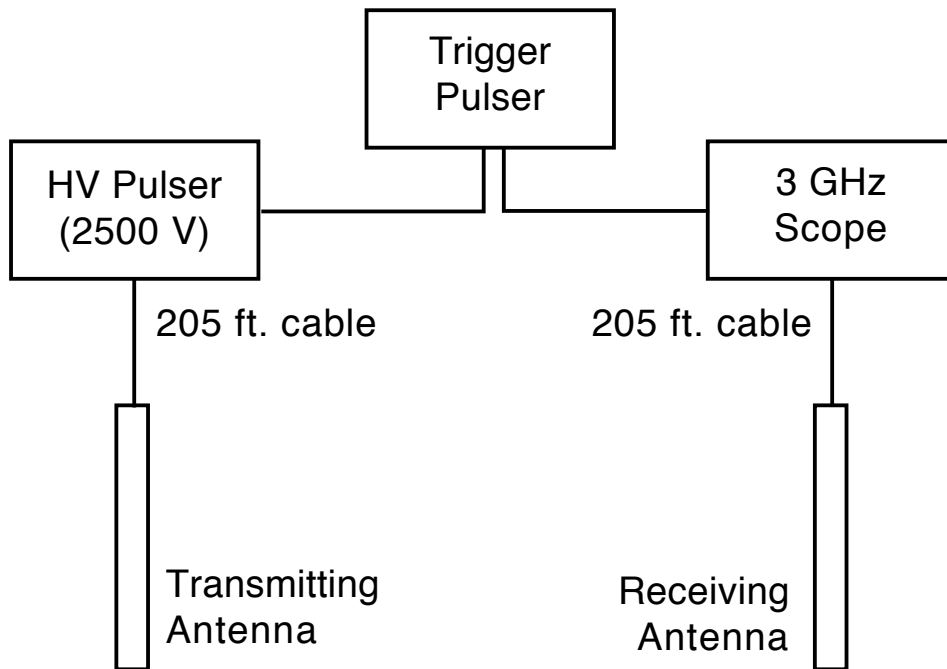


Fig. 2.

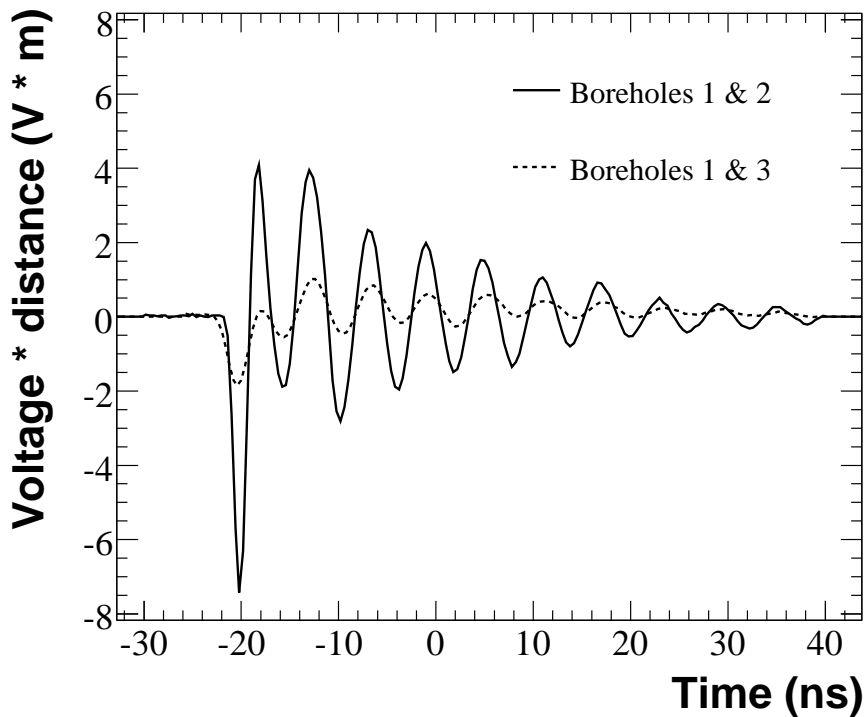


Fig. 3.

139 35 ns for the LF antennas, 30 ns for the MF antennas, and 12 ns for the HF
 140 antennas.

141 We expect to record reflections from interfaces within the salt and from the
 142 salt-air boundary. We were able to see reflections from the 1500 ft. corridor
 143 with the receiver at either borehole. The time window that we use to for the
 144 analysis extends no more than 20 ns after the peak of the pulse to ensure
 145 that we eliminate the possibility of interference from any reflection off of the
 146 corridor for depths of 50 ft. and deeper.

147 We sum the total power in frequency bands that are 50 MHz wide for the LF
 148 and MF antennas, and 100 MHz wide for the HF antennas which had a larger
 149 bandwidth. We subtract the noise contributions in each band. The noise power

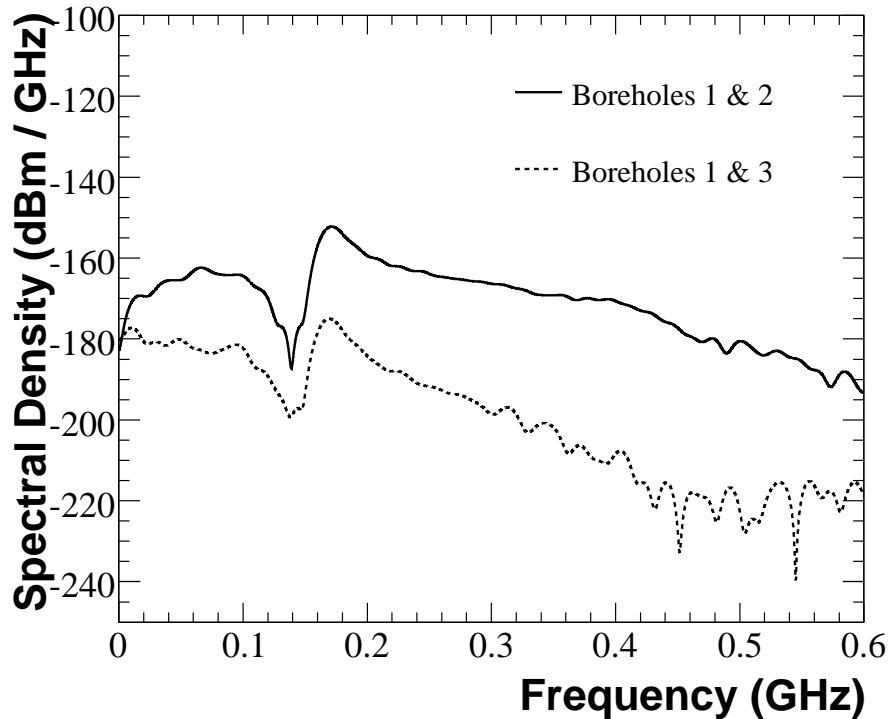


Fig. 4.

150 is taken from a sample waveform for each antenna type in a time window of the
 151 same length as the pulse window but earlier in time than any pulse appears.
 152 The noise subtraction had a small effect on the calculated attenuation length
 153 because the signal to noise ratio was high in the band of the antenna.

154 We define voltages V_{12}^i and V_{13}^i to be the square root of the power in the i^{th}
 155 frequency bin between Boreholes 1 and 2 and Boreholes 1 and 3 which span
 156 distances d_{12} and d_{13} respectively. Since we used the same system regardless
 157 of the location of the receiver, the voltages received in the boreholes from the
 158 transmitter are related by:

$$159 \quad \frac{V_{13}^i}{V_{12}^i} = \frac{d_{12}}{d_{13}} \cdot \exp \left[- (d_{13} - d_{12}) / L_{\alpha}^i \right] \quad (1)$$

160 where L_α^i is the field attenuation in the i^{th} frequency bin. Inverting this equa-
 161 tion gives an expression for the field attenuation length in each frequency
 162 bin:

$$163 \quad L_\alpha^i = (d_{13} - d_{12}) / \ln \left(\frac{d_{12} V_{12}^i}{d_{13} V_{13}^i} \right) \quad (2)$$

164 5 Uncertainties

165 The main source of systematic uncertainty on the measurement of the field
 166 attenuation length at a given depth is due to the position of the antenna
 167 within the hole. In previous trips to Cote Blanche, we discovered that a small
 168 variation in position of the antenna led to a significant change in the voltage
 169 received through the salt [13]. We estimate the size of this uncertainty as the
 170 root mean square variation between neighboring depths of the peak-to-peak
 171 voltage of the recorded waveform at each depth (excluding the 10 and 20 ft.
 172 depths):

$$173 \quad \delta V = \frac{1}{N} \sqrt{\sum_{i=0}^{N-1} (V_i - V_{i+1})^2} \quad (3)$$

174 where N is the number of depths included here. Using this method, we estimate
 175 the uncertainty on the voltage measured due to the position of the antenna in
 176 the hole to be 24%.

177 We also include an uncertainty due to the exact choice of the time window
 178 that contains the pulse. We estimate this uncertainty as the root mean square

179 variation of the total power in the pulse as we slide the time window by 1 ns.
180 When the power at a given frequency is small, this uncertainty dominates (up
181 to 50% in voltage), but in the frequency band of the antenna, the uncertainty
182 is small (less than 10% in voltage).

183 There is also an uncertainty on the distance between the holes. We measured
184 the distance between Boreholes 1 and 2 with a measuring tape, and then used
185 relative timing of received pulses to extrapolate the distance between Bore-
186 holes 1 and 3. The uncertainty on these distances include a contribution from
187 system timing (± 3 ns), one due to the measurement of the distance between
188 Boreholes 1 and 2 (± 1 ft.), and one due to a depth-dependent potential devi-
189 ation of the boreholes from vertical ($< \pm 3$ ft.). The maximum uncertainty on
190 the distance between the transmitting and receiving antennas is always less
191 than 2.1%.

192 **6 Results**

193 *6.1 Antenna Transmission*

194 Using the same pulser that was used for the attenuation measurements, we
195 measured the fraction of power reflected from each antenna while it was in
196 a borehole so that we could deduce the fraction transmitted and frequency
197 dependence. For this S11 measurement, we inserted a coupler (Minicircuits

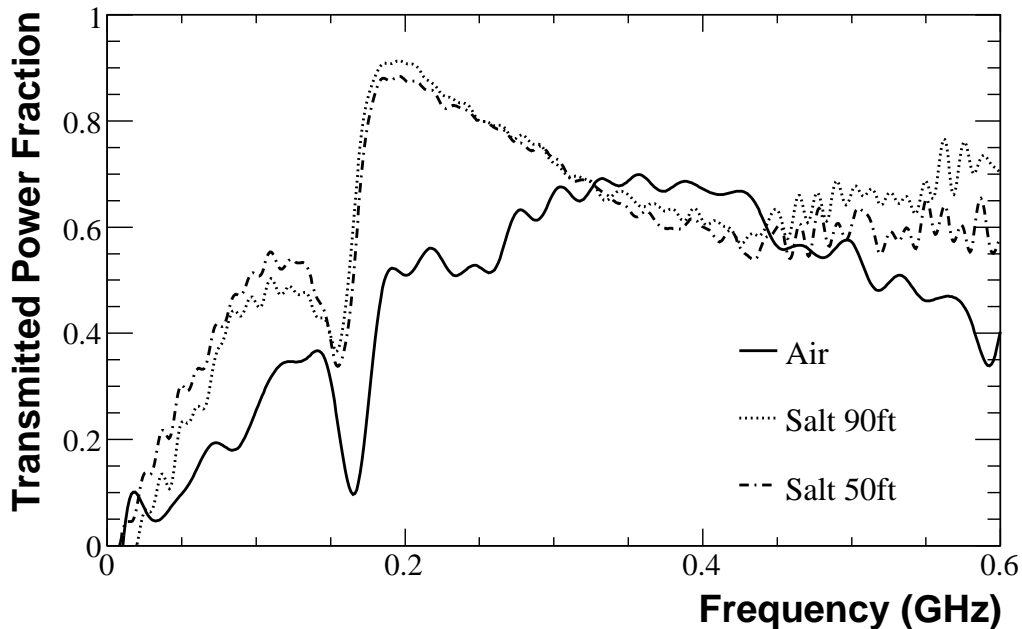


Fig. 5.

198 ZFDC-20-4) between the pulser and antenna and recorded the reflected signal
 199 through the coupled port. After measuring the reflection from the open cable
 200 (with the setup identical but with only the antenna removed), the ratio of the
 201 power in the two pulses is the fraction reflected from the antenna. The trans-
 202 mitted fraction is deduced by taking the sum of the reflected and transmitted
 203 power fractions to be unity. Figure 5 shows the transmission of an MF antenna
 204 as a function of frequency. The transmission did not change significantly when
 205 we changed the depth of the antenna in the hole.

206 6.2 Attenuation Lengths

207 Figure 6 shows the attenuation length in the frequency bin centered on 250 MHz
 208 as measured with the MF antennas plotted versus depth. We took measure-

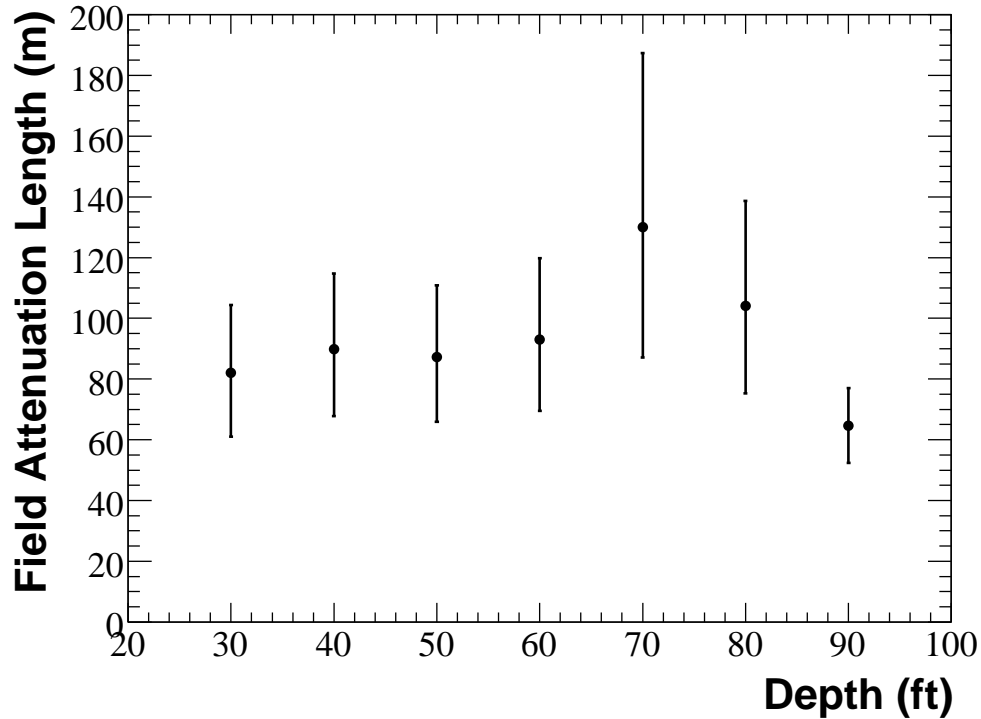


Fig. 6.

209 ments at 10 and 20 ft. depths, and the values we calculate for the attenua-
 210 tion length at those shallow depths are consistent with attenuation lengths
 211 at greater depths; however, we only report the results from 30 ft. and deeper
 212 since the deeper measurements are more likely to be of unfractured, clear salt.
 213 At 30 and 40 ft., as much as 1/4 of the power in the waveforms received at
 214 Borehole 3 may be due to power from a reflected pulse (based on measure-
 215 ments at greater depths) but we still include those points here. We do not
 216 observe a depth dependence in attenuation length.

217 Measured field attenuation length at 50 ft. and 90 ft. depths are shown in
 218 Figure 7 as a function of frequency. The LF antennas were not easily lowered
 219 beyond 75 ft. depth, so we include data from those antennas at 75 ft. instead

220 of 90 ft. If the salt had a constant loss tangent, we would expect that the
 221 attenuation length would decrease with increasing frequency as ν^{-1} , where ν
 222 is the frequency of the radiation [6]. We fit the points in Figure 7 to a power
 223 law of the form:

$$224 \quad L_{\alpha}(\nu) = a \cdot \left(\frac{\nu}{1 \text{ GHz}} \right)^b \quad (4)$$

225 and the best fit values are $a = 32 \pm 2$ m and $b = -0.57 \pm 0.06$, with a
 226 $\chi^2/\text{dof}=25.6/36$. Although it is clear that the attenuation length is falling
 227 with increasing frequency, it does not follow the ν^{-1} expectation, which hints
 228 at a non-constant loss tangent, consistent with measurements at the Hock-
 229 ley mine [6]. In Table I, we list the measured attenuation lengths at a few
 230 frequencies of interest based on the best fit values from this fit.

231 The uncertainties on the distances between the holes is one that would move
 232 the measured attenuation length in the same direction at all measurement
 233 positions, so we do not include them in the fit. The uncertainties on the
 234 distances between the holes are small compared to the remaining uncertainties.
 235 If we vary the distances by their uncertainties and refit, the attenuation lengths
 236 change at most by $\pm 2\%$.

237 We have also averaged the attenuation length at each frequency over all depths
 238 of 50 ft. and deeper and over all antenna types, and plotted the results in
 239 Figure 8. This figure also shows the best fit power law function, with best fit
 240 values $a = 31.1 \pm 0.3$ m and $b = -0.68 \pm 0.04$ with a $\chi^2/\text{dof}=13.3/12$. For this

241 plot the uncertainties only include the scatter between measured attenuation
242 lengths using different antennas and at different depths in the same frequency
243 bin.

244 The attenuation lengths that we measured on this trip are significantly longer
245 than those that we measured on our previous trip to the same mine. The
246 measurements that we report here were made in boreholes that were drilled
247 into the floor of the lowest level of the mine, whereas the previous measure-
248 ments were made with holes drilled into the ceiling and against the walls of
249 the corridors. Because the method of mining consists of cutting under the salt
250 and then blasting the wall above the cut, any fractures that occur due to the
251 process would tend to propagate upward. This means that the salt in the floor
252 of the lowest level of the mine would tend to be less fractured and probably
253 exhibit less loss in the radio regime due to scattering.

254 *6.3 Index of Refraction*

255 We also calculate the index of refraction of the salt using the direct trans-
256 mission measurements that we made. The index of refraction is defined as
257 $n = \sqrt{\epsilon'}$, where ϵ' is the real part of the dielectric permittivity. We calculate
258 the speed of transmission through the medium using the distance between
259 Boreholes 1 and 2 and the time of travel of the signal pulse through the salt.
260 The time of travel was measured by taking the difference between the time

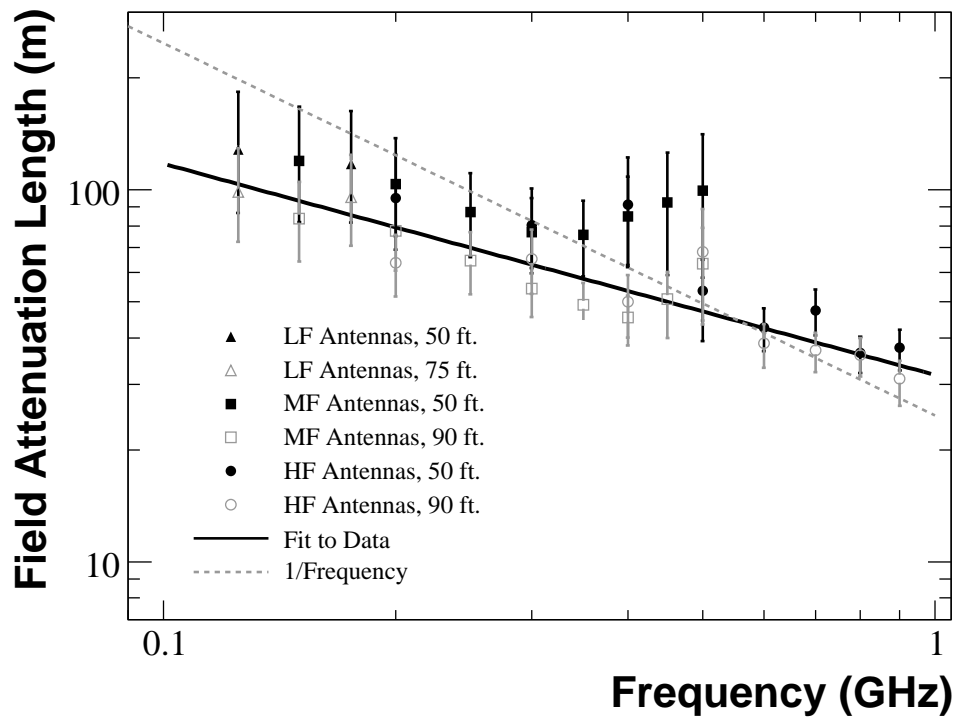


Fig. 7.

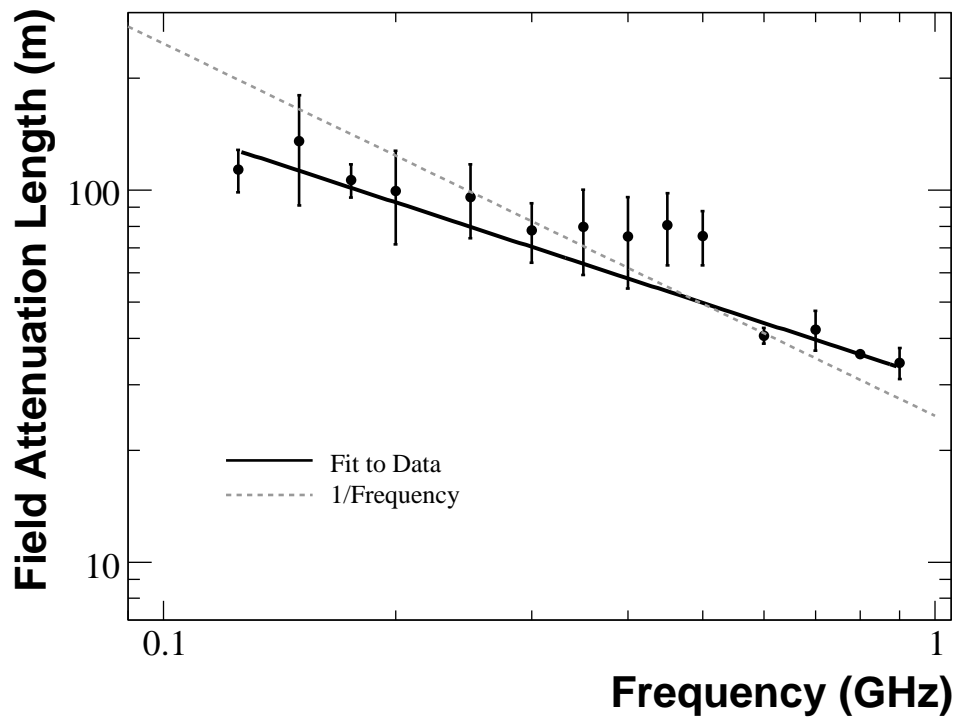


Fig. 8.

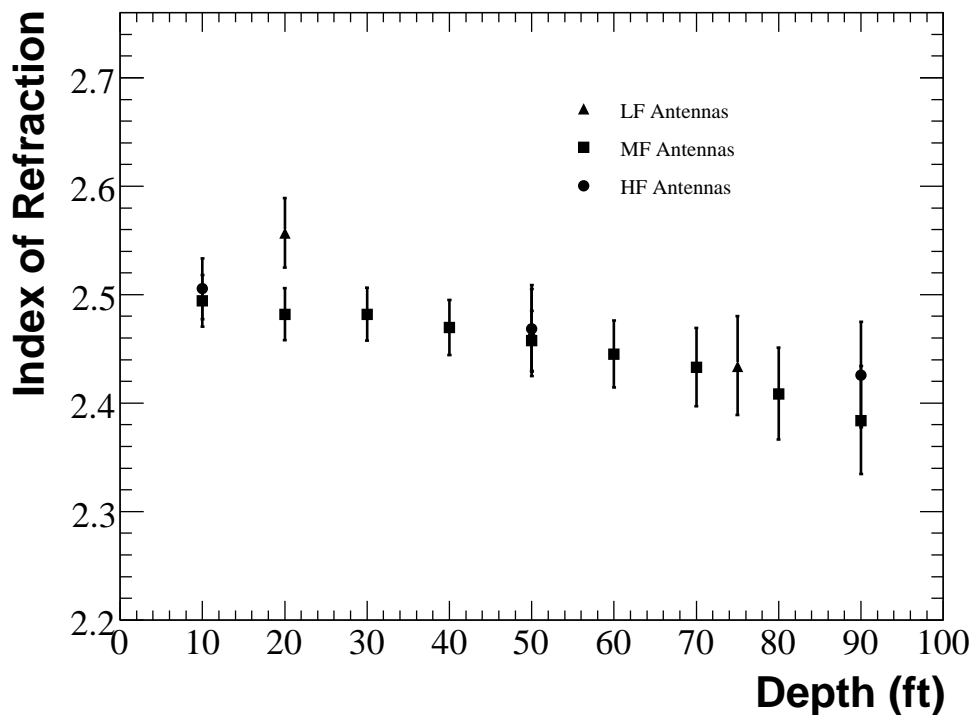


Fig. 9.

261 that the pulse was generated and the signal was received and subtracting the
 262 known system delay.

263 Figure 9 shows the measured index of refraction at each depth. The index of
 264 refraction that we measure is consistent with $n = 2.45$, the index of refraction
 265 of rock salt. We estimate an uncertainty of ± 3 ns on the absolute system
 266 timing and ± 1 ft. on the distance between the holes. We also include the same
 267 uncertainty due to potential deviation of the boreholes from vertical that was
 268 described in Section 5, which contributed $< \pm 3$ ft. to the uncertainty.

270 At nearly every measurement position we observed at least one clear “re-
271 flected” signal in addition to the “direct” signal that traveled along the straight
272 line between the transmitting and receiving antennas. Reflected signals can
273 be easily distinguished from direct signals from their time of arrival at the re-
274 ceiver. They allow us to probe distances greater than that between our drilled
275 holes, and to probe different salt regions as well. However, little is known
276 about the loss in power incurred at the reflection, and reflected signals are
277 often transmitted and received by the antennas at oblique angles, where the
278 antenna response is less well understood.

279 With our antennas in Boreholes 1 and 2, the entirety of the shortest path
280 between the receiver and transmitter was below the corridor where we were
281 working, so we expected to see reflections from that corridor. We did observe
282 signals that were consistent with this interpretation. The measured time dif-
283 ferences between the direct and reflected signals while we were transmitting
284 between Boreholes 1 and 2 were within approximately 10 ns of the expected
285 time difference at all depths. These reflected pulses traversed as much as 256 ft.
286 (78 m) of salt, and a discrepancy of 10 ns corresponds to approximately 4 ft.
287 (1.2 m) in salt. With the antennas at the greatest depths, Most of the power
288 in these reflected signal were out of the band of the antenna. We conclude that
289 this power was reflected off of the input of the antenna and radiated from the

290 feed cable which was acting as a long-wire antenna. In addition, the expected
291 beam pattern of a long-wire antenna is consistent with the angle of emission
292 seen with these reflections.

293 With our antennas in Boreholes 1 and 3, the specular path of a reflection
294 from the corridor level is not incident on a salt-air boundary, but nevertheless
295 at depths greater than 50 ft. (where the reflections did not interfere with
296 the direct signal) we did observe signals whose timing were consistent with
297 reflections from the corridor level within 10 ns. In addition, with the antennas
298 in Boreholes 1 and 3 we observed signals at all depths 30 ft. and deeper
299 consistent with having reflected from 170 ft. above the corridor where we
300 stood. The 1300 ft. level of the mine is of course nominally 200 ft. above the
301 floor of the corridor. Therefore, we observed signals having traveled through
302 as much as 624 ft. of salt when the MF antennas were 90 ft. and 150 ft. deep.

303 *6.5 Beam pattern in salt*

304 The deep holes provided to us by the Cote Blanche mine presented a unique
305 opportunity to measure the beam pattern of our antennas while completely
306 submerged in salt, although due to the distances involved, we did not probe a
307 broad range of angles. With one MF antenna at 90 ft. depth in Borehole 1, we
308 took data with the second MF antenna in Borehole 2 and at depths of 20 ft.,
309 50 ft., 70 ft. and 90 ft., and in Borehole 3 at depths of 90 ft., 130 ft. and 150 ft.

310 The waveform at 20 ft. depth contained interference from a reflected signal, so
 311 that data was not included in this measurement. The remaining data probed
 312 the antenna beam pattern at angles of -6.2° , -4.1° , 0° , 7.0° and 13.8° with
 313 respect to the horizontal, defined to be positive when the antenna in Borehole 1
 314 was deeper than the antenna in the other borehole. After correcting for $1/r^2$
 315 power loss as well as salt attenuation loss based on our measured values, we
 316 plot the measured power at each position relative to that measured at 0° in
 317 the same borehole. We use the same uncertainties as described in Section 5.
 318 The solid line in the figure is the expected beam pattern for a half-wave dipole
 319 in air:

$$320 \quad \frac{dP_{\text{Rel}}}{d\Omega} \propto \left[\frac{\cos\left(\frac{\pi}{2} \cdot \sin\theta\right)}{\cos\theta} \right]^2. \quad (5)$$

321 Although our uncertainties are large, we do not see a deviation from the half-
 322 wave dipole beam pattern. The data is also not inconsistent with the peak of
 323 the transmission being in the horizontal direction.

324 **7 Review of Ground Penetrating Radar Data**

325 Ground Penetrating Radar (GPR) measurements were made in the Cote
 326 Blanche mine and other salt mines in the 1970's by Stewart and Unterberger
 327 [7,14] to probe discontinuities in the salt and the location of the top of the
 328 dome. They used a single frequency waveform generator at 440 MHz, a pair

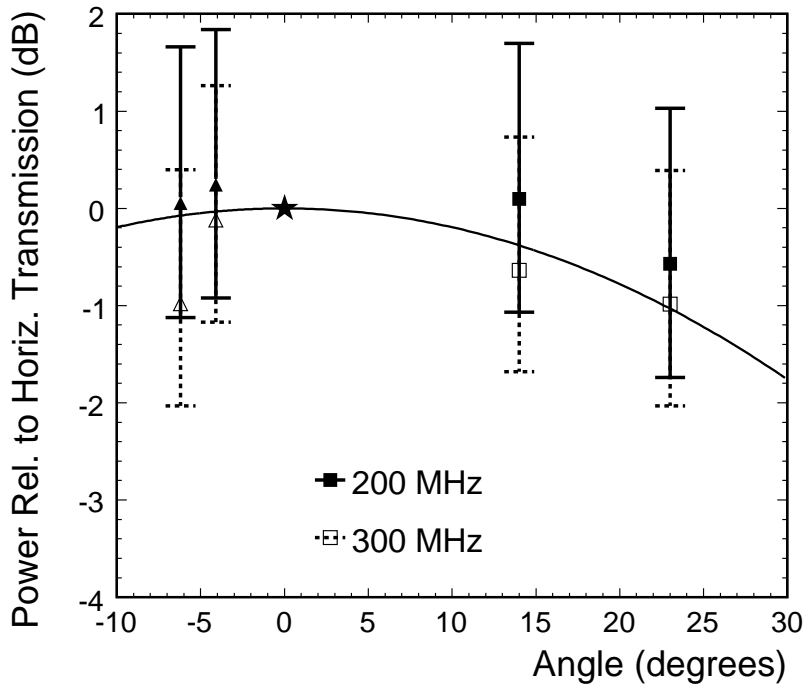


Fig. 10.

329 of high-gain antennas that were pointed into the salt of interest, and an os-
 330 cilloscope to measure the time delay between the transmitted signal and any
 331 received reflections off of discontinuities deep within salt. To calculate the
 332 distance of the discontinuities, they used an index of refraction measured via
 333 transmission across a pillar of salt (their result implies $n = 2.62$).

334 They measured the location of the top of the Cote Blanche dome from within
 335 the mine by transmitting the signal vertically through the ceiling. Although
 336 the paper reports that attenuation of 2-3 dB per 100 ft. is typical for radar in
 337 dry salt in general, which would imply field attenuation lengths in the range
 338 90-140 m, at one measurement station they report a multiply-reflected signal
 339 that had traveled through a total path length of 4080 ft. (1244 m) and stated

340 that it was the longest transmission distance observed in any mine. We have
341 compiled information in Table II from the discussion of the specifications of
342 the system used to make the measurements in References [7] and [14].

343 The power received, P_{Rx} , is related to the power transmitted, P_{Tx} , by the Friis
344 formula:

$$345 \quad P_{Rx} = P_{Tx} \frac{G_{Tx} G_{Rx} \lambda^2}{(4\pi r)^2} \quad (6)$$

346 where G_{Tx} and G_{Rx} are the gain of the transmitting and receiving antennas,
347 λ is the wavelength of the transmitted signal in salt, and r is the distance
348 between the antennas. Using the result of the Friis formula together with the
349 GPR system specifications, we estimate that the minimum attenuation length
350 allowed to detect the reflected signal over the longest distance observed (see
351 Table II) is 138 m, assuming that they detected the signal just at the sensitivity
352 threshold of their system.

353 This attenuation length is not inconsistent with some of our measurements in
354 the same frequency range, although our results show generally higher losses.
355 Note that if there are variations in the clarity of the salt, the longest observed
356 path length quoted in their paper would be more likely to be from the clearest
357 salt that they had sampled among all of their measurements. We only sampled
358 one section of salt with these measurements.

359 In order to replicate the low-loss results of the GPR technique, any further

360 measurements would have to be made with a portable high-power system
361 capable of making measurements at many locations.

362 We made a brief attempt at making measurements using the GPR technique
363 during our visit to the mine. Using the same high-power pulser and oscillo-
364 scope, we used a pair of directional antennas in an attempt to see reflections
365 off of interfaces within the walls of the mine. We did see late reflected pulses,
366 but we did not understand that data well enough to conclude whether the
367 reflections that we saw came from within the salt, or were merely reflections
368 down the corridor of the mine.

369 8 Simulation

370 We have run a simulation to estimate the sensitivity of an array of antennas
371 embedded in salt with the attenuation lengths that we have measured here.
372 As much as possible, we use the same parameters as the simulated array
373 described in the Hockley paper for direct comparison [6]. The simulated array
374 consists of $10 \times 10 \times 10$ dipole antennas with center frequency at 150 MHz and
375 50% bandwidth in a salt formation that is a cube 4 km on a side. We require
376 4 antennas hit with a signal-to-noise ratio of 4σ . The previous study in [6]
377 considered a 300 m attenuation length at 300 MHz and a $1/\nu$ dependence,
378 whereas we have measured a 63 ± 3 m attenuation length at 300 MHz and the
379 spectral index that we measure is -0.57 ± 0.06 . Reproducing the simulated

380 Hockley array, we expect 12 events per year compared to the order 10 events
381 per year that they quote in their paper. Using the measured Cote Blanche
382 attenuation lengths, we expect 1.4 events per year ultra-high energy neutrino
383 flux [2], for a factor of 9 reduction in sensitivity due to a lower measured
384 attenuation length, but still a non-negligible rate over a one year run time.

385 9 Conclusions

386 We have measured field attenuation lengths in the frequency range 125-900 MHz
387 using broadband pulses transmitted and received by dipole antennas in bore-
388 holes drilled 100 ft. into the floor of the 1500 ft. deep level of the the Cote
389 Blanche salt mine. The best fit power law that describes the measured frequency-
390 dependent attenuation lengths is given by

$$391 \quad L_{\alpha} = (32 \pm 2) \cdot (\nu/1 \text{ GHz})^{-0.57 \pm 0.06} \quad (7)$$

392 with statistically dominated uncertainties. This is the most precise measure-
393 ment of radio attenuation in a natural salt formation to date.

394 The main result of this paper is derived from data that we took on our third
395 trip to the Cote Blanche Salt Mine. The data taken from the three trips
396 indicates that the room and pillar system of mining leads to regions of salt
397 near the walls and ceilings of the corridors with short attenuation lengths
398 (~ 10 m) which could be due to fracturing brought about by the explosives

399 used in that method. We find that the salt that is just under the floor of a
400 corridor does not suffer the same degradation, which may be due to the cut
401 along the floor that is made prior to the detonation of the explosives to blast
402 away the salt.

403 Although we expect there to be variation in salt properties between salt domes
404 as well as regions of salt within the same dome, we have compared our measure-
405 ments with previous measurements made at Cote Blanche and elsewhere. Our
406 result is not inconsistent with attenuation lengths measured at the Hockley
407 Salt Mine. We have attempted to compare our measurements with the longest
408 transmission distance reported by GPR experts in the same mine. Our data
409 generally showed greater attenuation than can be reconciled with that result.
410 However, due to the variation observed in our data, some of our measurements
411 do point to salt that could have been clear enough to be consistent. That we
412 strain to reconcile our numbers with the longest transmission distance reported
413 there may indicate that there are regions of the Cote Blanche mine with salt
414 that has less attenuation than in the regions where our measurements were
415 made.

416 We have modeled a SalSA array of $10 \times 10 \times 10$ dipole antennas in boreholes
417 that reach 3 km depth to assess the sensitivity of a neutrino detector in salt
418 with the attenuation lengths that we report here to compare with the simu-
419 lation study described in the Hockley attenuation length paper. We find the
420 lower best fit attenuation lengths measured at Cote Blanche reduce the sen-

421 sitivity of such a detector measured in terms of event rate by a factor of 9,
422 but still maintain an expectation of order one event per year using a standard
423 model for the expected ultra-high energy neutrino flux.

424 In order for a next-generation neutrino detector in salt that measures \sim
425 10 GZK events/year to be feasible, attenuation lengths longer than the \sim
426 100 m lengths reported here will likely be necessary. However, since this re-
427 sult is based on a limited region of the dome, and past GPR results in the
428 same mine may have pointed clearer salt, there are reasons to be optimistic
429 that there is clearer salt in other locations whose radio loss has not yet been
430 precisely measured. For this to be pursued further, we believe that developing
431 a portable radar system is a compelling next step so that the radio loss of the
432 salt can be sampled in many locations on a single visit to a mine.

433 **10 Acknowledgements**

434 We are grateful to mine manager Gordon Bull at the North American Salt
435 Company for supporting our project and his generosity in permitting us to
436 carry out this work in the Cote Blanche mine on three separate visits. We
437 would also like to thank Scott Fountain, Robert Romero and the other miners
438 at Cote Blanche that provided us with constant assistance on our visits to
439 make these measurements a success, and for drilling custom boreholes for us
440 which make these measurements unique in the world. We would also like to

441 thank the High Energy Physics Division of the U.S. Department of Energy,
442 the U.K. Particle Physics and Astronomy Research Council and the Royal
443 Society for funding this project.

444 **References**

- 445 [1] G. T. Zatsepin and V. A. Kuzmin, JETP Lett. **4**, 78 (1966). [Pisma Zh. Eksp.
446 Teor. Fiz. **4**, 114 (1966)]; K. Greisen, Phys. Rev. Lett. **16**, 748 (1966).
- 447 [2] R. Engel et al., Phys. Rev. D **64**, 093010. For a standard expectation of a
448 neutrino flux from the GZK process, we take the component from electron
449 neutrinos from Figure 4 and for the muon neutrino contribution we take the
450 upper curve of Figure 9.
- 451 [3] S. Barwick, et al., J. Glaciology **51**, 231 (2005).
- 452 [4] G. Askaryan, Soviet Physics JETP-USSR **14** (2), 441-443 (1962).
- 453 [5] D. Saltzberg et al. Phys. Rev. Lett. **86**, 2802-2805 (2001); P. Gorham et al.
454 Phys. Rev. D **72**, 023002 (2005); P. Gorham et al. Phys. Rev. Lett. **99**, 171101
455 (2007).
- 456 [6] P. Gorham, D. Saltzberg et al., Nucl. Instrum. Meth. **A** 490, 476-491 (2002).
- 457 [7] R.D.Stewart and R.R.Unterberger, Geophysics **41** (1), 123-132 (1976).
- 458 [8] M. Halbouty, Salt Domes: Gulf Region, United States and Mexico, Gulf
459 Publishing Co., Houston, TX (1967).

- 460 [9] B. Lock and D.H. Kupfer, Salt Mines of South Louisiana, Louisiana Geological
461 Survey, Guidebook Series No. 7, 2003.
- 462 [10] M. Cherry, SalSA Collaboration Internal Note #22 (2005).
463 <http://bugs.physics.ucla.edu:8080/salsa/22>
- 464 [11] D. Wieczorek, SalSA Collaboration Internal Note #21 (2005).
465 <http://bugs.physics.ucla.edu:8080/salsa/21>
- 466 [12] A. Connolly, A. Goodhue, M. Cherry, and J. Marsh, SalSA Collaboration
467 Internal Note #38 (2006). <http://bugs.physics.ucla.edu:8080/salsa/38>
- 468 [13] A. Connolly, A. Goodhue, D. Saltzberg, SalSA Collaboration Internal Note #39
469 (2006). <http://bugs.physics.ucla.edu:8080/salsa/39>
- 470 [14] R.R.Unterberger, Geophysical Prospecting **26** (2), 312-328 (1978).

471 Figure 1. Map showing section of 1500 ft. level of the mine where we made
472 our measurements at Boreholes 1, 2, and 3. The letters and numbers follow
473 the naming system for the corridors used by the mine. The hatched regions
474 are the salt surrounding the corridors.

475 Figure 2. System diagram.

476 Figure 3. Pulses that propagated directly between the transmitter and receiver
477 between Boreholes 1 and 2 between Boreholes 1 and 3 using the MF antennas
478 at a depth of 90 ft. We plot voltage multiplied by the distance between trans-
479 mitter and receiver for each pulse, which should be constant in the absence of
480 any attenuation.

481 Figure 4. Fourier transforms of pulses in Figure 3.

482 Figure 5. Measured transmission for the custom-made MF antennas.

483 Figure 6. Attenuation length at 250 MHz measured with the MF antennas.
484 The uncertainties are smaller for shorter attenuation lengths since variations
485 in voltage have less of an impact when greater loss is observed.

486 Figure 7. Attenuation length shown as a function of frequency for two depths
487 and all three pairs of dipoles.

488 Figure 8. Average attenuation length, shown as a function of frequency. The
489 uncertainties shown in this plot are the scatter of the measured attenuation
490 lengths using different antennas and at different depths.

491 Figure 9. Index of refraction measured at each depth.

492 Figure 10. Measurement of beam pattern while one MF antenna was at 90 ft.

493 depth in Borehole 1 and the other was at various depths in Borehole 2 or 3.

494 The square markers are measurements taken with the second MF antenna

495 in Borehole 2 and the triangular markers with the second MF antenna in

496 Borehole 3. The star denotes 0 degrees, where the attenuation is by definition

497 0 dB.

Table I

Measured attenuation lengths at a few frequencies of interest based on fitting the data at 50 ft. and 90 ft. depths to the power law function as described in the text.

Frequency (MHz)	Measured Attenuation Length (meters)
150	93 ± 7
300	63 ± 3
440	51 ± 2
900	36 ± 2

Table II

Specifications of the GPR system used in [7] and [14], and an estimation of the minimum attenuation length needed to see the longest path length reflection observed.

System Specifications		
Antenna Gain	17 dB	
Frequency	440 MHz	
Maximum Transmission Distance	1244 m	
Attenuation Length Estimation		
Peak Power Output	40 dBm	10 W
Loss from transmission (from Friis formula)	61 dB	1.3×10^6
Power received (assuming no attenuation)	-21 dBm	8.0×10^{-6} W
System Sensitivity	-100 dBm	10^{-13} W
Maximum attenuation allowed	-79 dB	1.3×10^{-8}
Attenuation length	> 138 m	